EFFECT OF TEMPERATURE GRADIENT NEAR THE TARGET AND GAS FLOW RATE ON THE DIAMETER DISTRIBUTION OF SINGLE-WALLED CARBON NANOTUBES GROWN BY THE LASER ABLATION TECHNIQUE

Rahul Sen[1], Hiromichi Kataura[2], Yohsuke Ohtsuka[1], Toshinobu Ishigaki[1], Shinzo Suzuki[1] and Yohji Achiba[1]
[1]Department of Chemistry, Tokyo Metropolitan University, Tokyo 192-0397, JAPAN
[2]Department of Physics, Tokyo Metropolitan University, Tokyo 192-0397, JAPAN

ABSTRACT

Gas dynamic and time resolved imaging studies have been performed on the growth of single-walled carbon nanotubes (SWNTs) in the laser ablation process. SWNTs were synthesized by laser ablation of Ni-Co catalyzed graphite targets at 1200 ^{o}C under argon gas. The effects of the temperature gradient near the target and the gas flow rate were studied in order to understand the effect of gas dynamics over the diameter distribution of SWNTs. The gas flow rate affects the diameter distribution of SWNTs especially when the growth species flow through a large temperature gradient. Scattering images from the growth species at different flow rates was recorded by high-speed video imaging. The results indicate that the velocities of these species are dependent on the gas flow rate but this dependence is evident 30 ms after the laser ablation. These findings are used to estimate the time period for the nucleation and the growth of SWNTs.

INTRODUCTION

Electronic properties of single-walled carbon nanotubes (SWNTs) depend crucially on their structural parameters such as diameter and chirality [1]. It is important to understand the growth mechanism of SWNTs to achieve a control over their diameter distribution and to produce nanotubes of desired property. Laser ablation of metal-graphite composite targets in argon gas can produce high quality SWNTs, however the diameters and chiralities of the nanotubes vary considerably for a given set of growth conditions [2-4]. Bandow et al. [5] reported that the mean diameter of the nanotubes increased with increasing temperature of the growth environment in laser ablation. Diameters of SWNTs can also be changed by changing the catalyst system [6] or by changing the catalyst ratio [7]. Despite these reports the process and mechanism of SWNT growth is not well understood. We consider that by changing various control parameters in the laser ablation process and by studying the dynamics of the ablated species, we can obtain an insight into the growth process of the SWNTs. We have studied the effect of the temperature gradient around the target and the gas flow rate on the diameter distribution of SWNTs. We also observed the scattering images of the laser-ablated species recorded by time-resolved photography. We estimated the velocities of the species inside the furnace and correlated them with the flow rates. Finally, the effect of the flow rate on the diameter distribution of SWNTs and the actual flow rate of the species are used to estimate the nucleation and growth times of SWNTs.

EXPERIMENTAL

SWNTs were grown by the laser ablation of metal-graphite composite targets using the metal catalysts, Ni(0.6 at.%)-Co(0.6 at.%). The target was supported by a graphite holder and fixed to a rotating molybdenum rod inside a quartz tube. A rotary pump first evacuated the

quartz tube, and then flowing argon gas was introduced into it. The pressure of argon gas inside the tube was maintained at 500 Torr and the flow rate was set to a desired value. An electric furnace heated the quartz tube, and the temperature was maintained at 1200 ^{o}C. Laser ablation was carried out by using the second harmonics of a Nd:YAG laser (532 nm, 10 Hz), focused to a 5 mm diameter spot on the target. The laser power was 300 mJ/pulse, and the ablation was carried out for 30 min. During the laser ablation the flowing argon gas carried the carbon products downstream, where a mat-like material was found to deposit on the molybdenum rod near the outlet region of the furnace. This material was collected by scraping and analyzed by Raman spectroscopy and transmission electron microscopy (TEM). Raman scattering was measured using a 1 m double monochromator, Jobin Yvon U-1000, and a photo-multiplier, Hamamatsu Photonics R943-02. The laser excitation line for Raman spectroscopy was 488 nm, and the spectral resolution was 4 cm^{-1}. The diameter distribution of the SWNTs was analyzed from the Radial Breathing Mode (RBM) of the Raman spectrum.

Diameter-selective Raman scattering for SWNTs is important for the Raman band at about 180 cm^{-1}, which is associated with the RBM of the carbon nanotube [8]. According to theory the RBM frequency is inversely proportional to the diameter of SWNT [5]. The observed RBM bands of SWNTs could be fitted by a sum of multiple Lorentzian peaks. Two constraints were used for the fitting procedure as follows. Peaks were first selected by inspection; five Lorentzian peaks with widths ranging from 5 to 12 cm^{-1} were found to fit the experimental data reasonably well. Then all the peaks were given an equal width, and the fitting was repeated. A width of 8.4 cm^{-1} gave a good fit to the observed data. Each of the five peaks corresponds to the RBM frequency of SWNT having a particular diameter, and the tube diameter is inversely proportional to the RBM frequency. The relative yield of each SWNT was obtained by dividing the area of the corresponding RBM peak to the total area of all the RBM peaks. The RBM frequencies shown in Fig. 1 indicate that the SWNTs have diameters ranging from 1.1 to 1.5 nm. This was also confirmed by TEM observation. For confirmation of the appropriateness of correlating the intensities of the RBM peaks to the relative yields of SWNTs, it is important to consider resonance effects. The intensity of the RBM peaks is enhanced when the photon energy of the excitation laser is in resonance with an allowed optical transition between van Hove singularities in the electronic structure of SWNTs [8]. Resonance Raman scattering for an excitation wavelength of 488 nm occurs for semiconducting SWNTs with diameters of 1–1.6 nm due to the third and fourth van Hove singularities and for metallic tubes of about 0.8 nm diameter [9]. The diameters of SWNTs evaluated from the peak positions of the RBM frequencies for our samples fall in the range of 1.1–1.5 nm. Therefore, the detected RBM modes are of the semiconducting SWNTs of this diameter range. This enables a direct comparison of the RBM intensities and correlation of these intensities to the relative yields of the SWNTs.

Scattering images from the laser ablated species were recorded as follows. The ablation pulse was the fundamental of Nd-YAG laser (1064 nm, ~10 ns pulse width), and the scattering images were observed due to the second harmonic (532 nm, long pulse mode ~200 μs pulse width) operating at a fixed time delay. The ablation and scattering lasers were co-axial, and the images were collected at a direction perpendicular to them. The images were recorded by a high-speed video camera (Kodak Ektapro HS motion analyzer 4540), and the recording rate was 9000 frames/s (~100 μs time window for each frame).

RESULTS AND DISCUSSION

Changing the target position with respect to the center of the furnace changed the temperature gradient near the target and this is schematically represented in Figure 1. The

temperature profile inside the furnace, shown in Figure 1(b), indicates that a significant temperature gradient exists at positions far away from the center of the furnace. We have examined the effect of the target position on the diameter distribution of SWNTs and the details are discussed elsewhere in the literature [10]. In brief, the relative yields of the small-diameter SWNTs increases whereas that of large-diameter SWNTs decreases as the target is placed away from the center of the furnace. Since the ambient temperature away from the furnace center is lower than that at the center position, this finding suggests that lower ambient temperature favors the growth of SWNTs having smaller diameters. This result is consistent with the earlier report on the effect of ambient temperature on the diameter distribution of SWNTs [5].

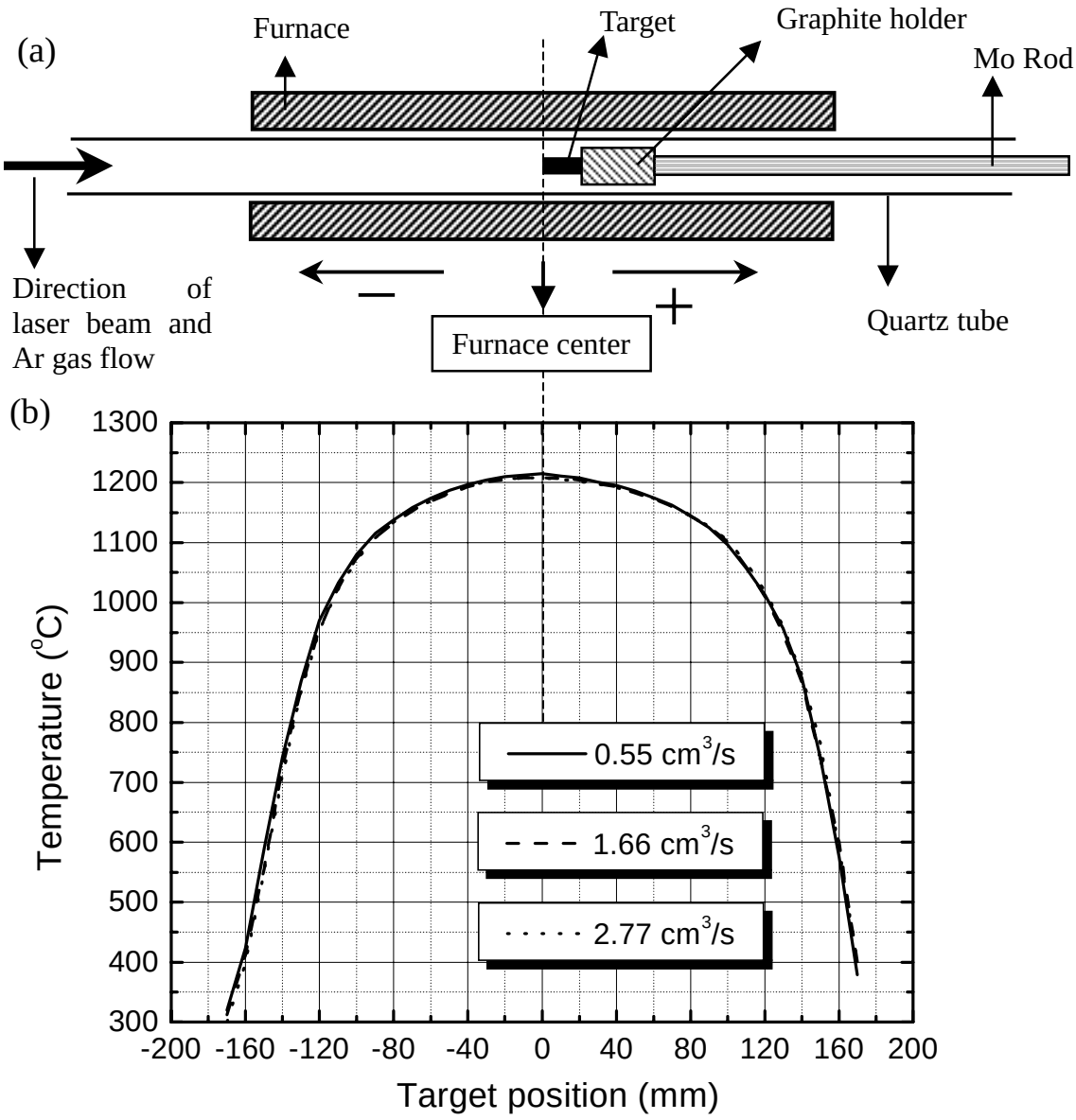

Figure 1 (a) Schematic representation of the experimental set-up for changing target position inside the furnace. When target is placed at the center it is termed as 0; when placed upstream it is negative and when placed downstream it is positive. (b) Temperature profiles inside the furnace at different gas flow rates.

After establishing the fact that the ambient temperature around the target is important for controlling the relative yield of SWNTs having different diameters, we studied the effect of gas flow rate on the diameter distribution of SWNTs. Figure 2 presents the Raman spectra associated with RBM of the SWNTs grown at different target positions under different flow rates. When the target was placed at the furnace center, the flow rate had only a small affect on the diameter distribution (Figure 2(a)). When the target was placed at –40 and –80 mm, however, the flow rate strongly affected the relative yields of SWNTs having different diameters (Figure 2(b) and (c)). In both cases, the intensity of the 163 cm^{-1} peak increased and that of the 203 cm^{-1} peak decreased with increasing flow rate. In other words, an increase in the flow rate increased the relative yields of large-diameter SWNTs and decreased the yields of small-diameter SWNTs. In the 0 mm case, the temperature gradient around the target was uniform (see Figure 1(b)), and the diameter distribution was essentially unaffected by the flow rate. In the –40 and –80 mm cases, however, the temperature gradient around the target was larger and the relative yields of SWNTs were more sensitive to the flow rate.

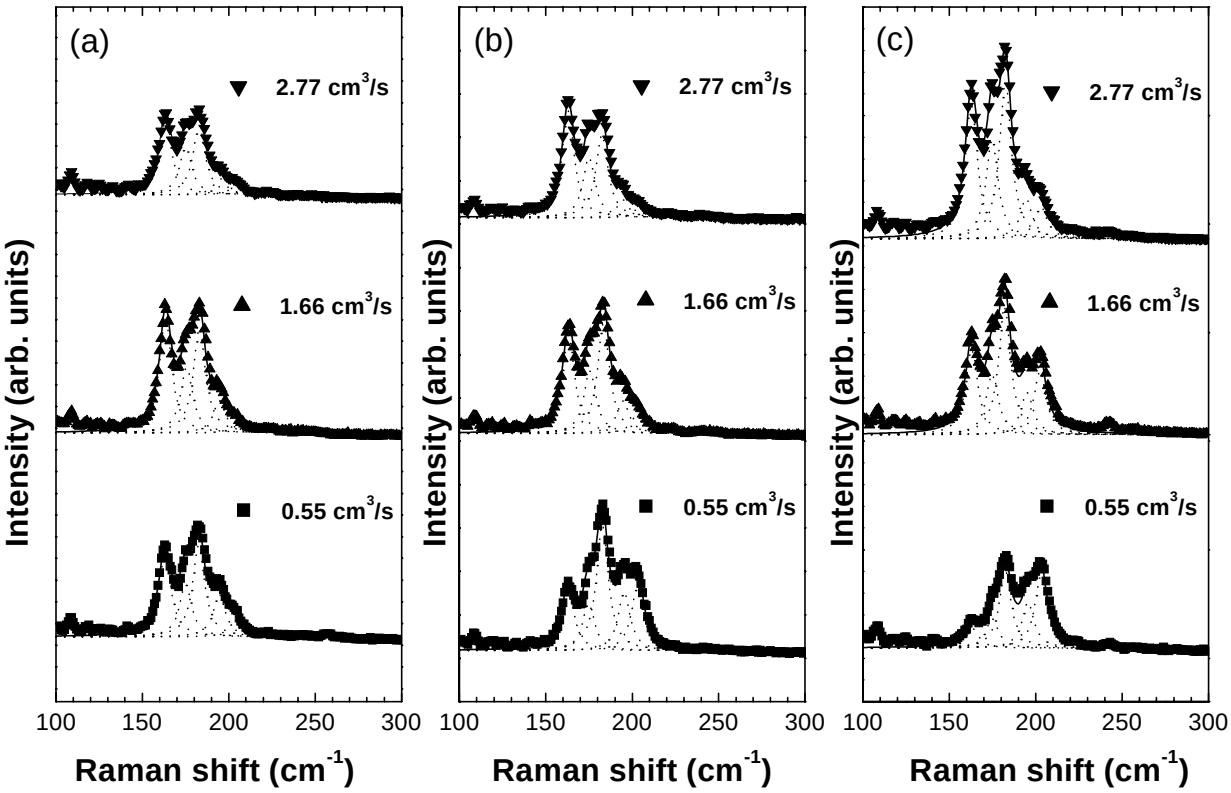

Figure 2. Raman spectra (RBM) of SWNTs grown at different target positions under different gas flow rates. The dotted curves represent the individual lorentzians, and the solid curve represents fit to the experimental data. Target positions are (a) 0 mm (furnace center), (b) –40 mm and (c) –80 mm.

To understand this flow rate effect, we recorded the scattering images of the laser ablated species at different flow rates. A series of photographs taken by a high-speed video camera at different time intervals after the laser ablation is shown in Figure 3. From the top frames in Figure 3, it is clear that 10 ms after the ablation the ablated species has moved about 40 mm from the target, and this distance is independent of the flow rate. This initial movement, caused by the ablation process, is in opposite direction to the gas flow and is termed forward movement. Images taken after 30 and 50 ms show that the particles have started moving in the direction of the gas flow, termed backward motion. From these time-resolved scattering images, the velocities of the backward moving species are estimated to be about 38, 123 and 255 mm/s for the flow rates of 0.55, 1.66 and 2.77 cm^3/s respectively. Since the velocities of the backward moving species increases with the flow rate, their positions inside the furnace after a certain time interval are different. This is clear from the bottom frames in Figure 3, 90 ms, for different flow rates. When the target is placed at the center, this difference in position of the backward moving species at different gas flow rates does not correspond to a large change in the temperature inside the furnace. When the target is placed at –40 or –80 mm, however, this difference means that after about 100 ms the backward moving species are at a much higher temperature when the flow rate is higher. Since a higher flow rate gives higher yields of SWNTs having larger diameters, it indicates that the temperature of the growth species is higher at a higher flow rate. This suggests that the SWNT growth process continues to occur even 100 ms after the laser ablation. Thus the growth period is long enough for the flow rate to significantly influence the relative yields of SWNTs having different diameters, especially when the growth species flow through a large temperature gradient.

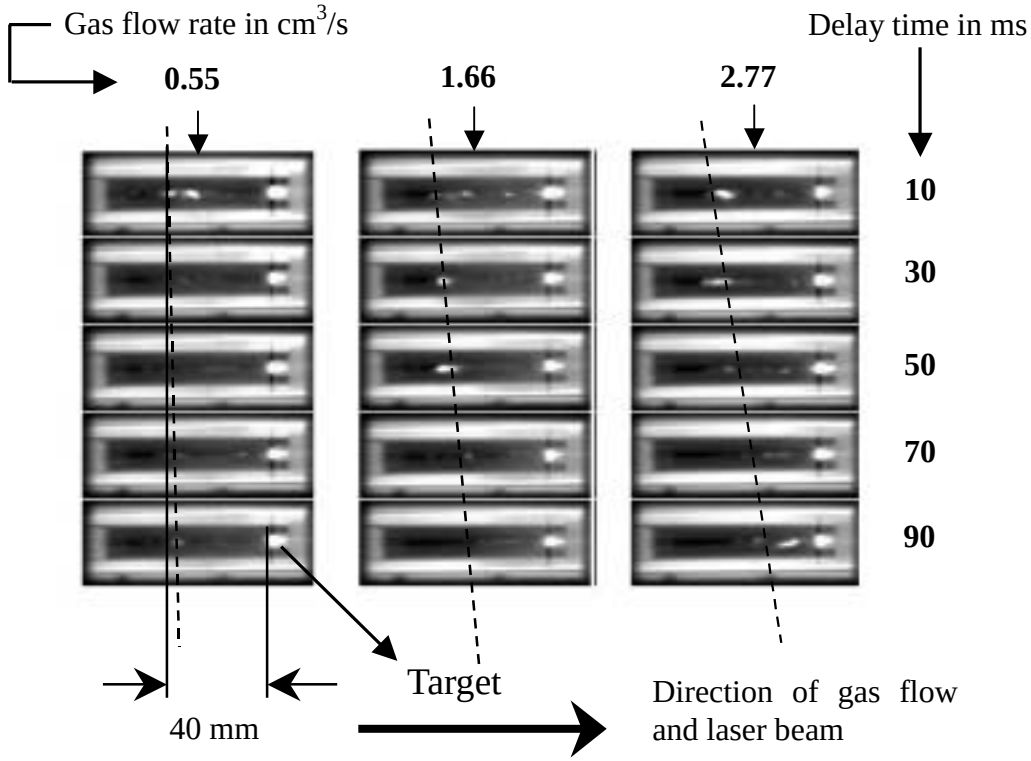

Figure 3. Scattering images from the laser ablated species recorded at different time intervals after the ablation pulse. The dashed line is given as a visual guide, showing the movement of the backward moving species with time.

CONCLUSIONS

Gorbunov et al. [11] studied the effect of the flow rate of argon gas on the overall yield of SWNTs; their results suggest that the growth times are of the order of 1 s. Recent studies of time-resolved imaging and spectroscopy on the dynamics of SWNTs growth process [12, 13] conclude that SWNTs' growth occurs in vortexes in long time periods (a few ms to a few s). Figure 2(b) and (c) show that the relative yields of large-diameter SWNTs increase with increasing flow rate whereas the overall range of the diameter distribution remains unaffected. Therefore, we conclude here that the initial condensation and nucleation processes, which may determine the range of diameter distribution, occur much faster (<100 ms) but the growth continues for about 100 ms and more.

ACKNOWLEDGEMENTS

This work was supported by the Japan Society for the Promotion of the Science (JSPS) (Research for the Future Program) and by the Ministry of Education, Science, Sports and Culture of Japan.

REFERENCES

1. M.S. Dresselhaus, G. Dresselhaus and P.C. Eklund, Science of Fullerenes and Carbon Nanotubes, Academic Press, San Diego, (1996) 802.
2. A. Thess, R. Lee, P. Nikolaev, H. Dai, P. Petit, J. Robert, C. Xu, Y.H. Lee, S.G. Kim, A.G. Rinzler, D.T. Colbert, G.E. Scuseria, D. Tomanek, J.E. Fischer and R.E. Smalley, Science 273 (1996) 483.
3. L-C. Qin, S. Iijima, H. Kataura, Y. Maniwa, S. Suzuki and Y. Achiba, Chem. Phys. Lett. 268 (1997) 101.
4. M.A. Pimenta, A. Marucci, S.D.M. Brown, M.J. Matthews, A.M. Rao, P.C. Eklund, R.E. Smalley, G. Dresselhaus and M.S. Dresselhaus, J. Mater. Res. 13 (1998) 2396.
5. S. Bandow, S. Asaka, Y. Saito, A.M. Rao, L. Grigorian, E. Richter and P.C. Eklund, Phys. Rev. Lett. 80 (1998) 3779.
6. H. Kataura, A. Kimura, Y. Ohtsuka, S. Suzuki, Y. Maniwa, T. Hanyu and Y. Achiba, Jpn. J. Appl. Phys. 37 (1998) L616.
7. O. Jost, A.A. Gorbunov, W. Pompe, T. Pichler, R. Friedlein, M. Knupfer, M. Reibold, H.-D. Bauer, L. Dunsch, M.S. Golden and J. Fink, Appl. Phys. Lett. 75 (1999) 2217.
8. A.M. Rao, E. Richter, S. Bandow, B. Chase, P.C. Eklund, K.A. Williams, S. Fang, K.R. Subbaswamy, M. Menon, A. Thess, R. E. Smalley, G. Dresselhaus and M.S. Dresselhaus, Science 275 (1997) 187.
9. H. Kataura, Y. Kumazawa, Y. Maniwa, I. Umezu, S. Suzuki, Y. Ohtsuka and Y. Achiba, Synth. Metals 103 (1999) 2555
10. R. Sen, Y. Ohtsuka, T. Ishigaki, D. Kasuya, S. Suzuki, H. Kataura and Y. Achiba, MRS Symposium Proceedings 593 (2000) 51.
11. A. A. Gorbunov, R. Friedlein, O. Jost, M. S. Golden, J. Fink and W. Pompe, Appl. Phys. A 69 (1999) S593.
12. F. Kokai, K. Takahashi, M. Yudasaka and S. Iijima, J. Phys. Chem. B 104 (2000) 6777.
13. A. A. Puretzky, D. B. Geohegan, X. Fen and S. J. Pennycook, Appl. Phys. A 70 (2000) 153.